

THE UNIVERSITY OF BRITISH COLUMBIA

DEPARTMENT OF STATISTICS

TECHNICAL REPORT #276

BY

Yanling Cai<sup>1</sup>, Jing Cai<sup>2</sup>, Jessica Chen<sup>1</sup>, Shirin Golchi<sup>2</sup>,  
Meijiao Guan<sup>1</sup>, Mohammad E. Karim<sup>1</sup>, Yang Liu<sup>1</sup>, Jabed  
Tomal<sup>1</sup>, Chao Xiong<sup>1</sup>, Yongliang Zhai<sup>1</sup>, Conroy Lum<sup>3</sup>,  
William J. Welch<sup>1</sup>, James V. Zidek<sup>1</sup>

<sup>1</sup> Department of Statistics, University of British Columbia

<sup>2</sup> Department of Statistics and Actuarial Science, Simon  
Fraser University

<sup>3</sup> FPInnovations, Vancouver, BC

February 2016

# An empirical experiment to assess the relationship between the tensile and bending strengths of lumber

Yanling Cai<sup>1</sup>, Jing Cai<sup>2</sup>, Jessica Chen<sup>1</sup>, Shirin Golchi<sup>2</sup>  
Meijiao Guan<sup>1</sup>, Mohammad E. Karim<sup>1</sup>, Yang Liu<sup>1</sup>,  
Jabed Tomal<sup>1</sup>, Chao Xiong<sup>1</sup> Yongliang Zhai<sup>1</sup>,  
Conroy Lum<sup>3</sup>, William J. Welch<sup>1</sup>, James V. Zidek<sup>1</sup>

<sup>1</sup> Department of Statistics, University of British Columbia

<sup>2</sup> Department of Statistics and Actuarial Science,  
Simon Fraser University

<sup>3</sup> FPInnovations, Vancouver, BC

Feb 2016

## Abstract

Setting structural engineering design values for lumber often involves a question of whether a sample is better utilized by testing one strength property with greater accuracy and precision, or splitting into two or more smaller samples to test multiple strength properties. This question can be solved by determining the relationship between strength properties. If their relationship is available, then not all the strength properties need to be tested as long as they are strongly related. In the summer of 2011, we conducted a proof load experiment in an industrial lab, to determine the dependence between lumber strength properties and their relationships. This paper first describes that experiment, and then presents an exploratory analysis of the data collected from the experiment. Major characteristics of lumber strength properties are learned through visualization, summary statistics and likelihood criterion.

# 1 Introduction

Setting structural engineering design values for forest products often involves a question of whether a quality monitoring sample is better utilized by testing one strength property with greater accuracy and precision, or splitting into two or more smaller samples to test multiple strength properties. A strong dependence between strength properties has important implications for the answer to this question. For it suggests that if there is a need to verify the strength properties, not all the strength properties need to be tested. The more expensive to measure strength property could be predicted from the other if the relationship between the strength properties is determined. This particularly means that the relationship between the strength properties could be exploited to reduce overall sampling costs in lumber long term monitoring programs. However, most strength properties are obtained by destructive tests. We are not able to observe the destructive strength properties on the same specimen.

In the summer of 2011, wood scientists at FPInnovations Lab in Vancouver, Canada and statisticians at the University of British Columbia conducted an experiment to “break a piece of lumber twice” (hereafter called the Summer – of – 2011 experiment). This Summer – of – 2011 experiment was designed to determine the relationship between ultimate tensile strength (*UTS*) and modulus of rupture (*MOR*). Both strength can only be measured by testing a lumber specimen to failure (destructive testing). Since the Summer – of – 2011 experiment used a technique called proof loading, it also allows us to quantify the damage accumulated in the strength caused by proof loading in the *UTS* or *MOR* mode. This paper is structured as follows. Section 2 introduces the Summer – of – 2011 experiment in great details. Section 3 explores the characteristics of the data collected from the Summer – of – 2011 experiment through visualization, summary statistics and likelihood criterion. The exploratory data analysis suggests distribution candidates for our next step: model the relationship between *MOR* and *UTS*. In Section 4, we summarize the design implemented in the Summer – of – 2011 experiment and the characteristics of lumber strength properties learnt from data.

## 2 The experiment

The Summer – of – 2011 experiment was based on the symmetric proof load design proposed by Amorim and Johnson [1]. The goal is to estimate the relationship between two destructive strength properties, ultimate tensile strength (*UTS*) and modulus of rupture (*MOR*). The *MOR* is the maximum bending stress that a specimen can sustain before failure, expressed in psi. The *UTS* is the maximum tensile stress in pounds per square inch (psi) that a specimen can sustain in a direction parallel to the grain (a texture produced by wood fibres; visible to eyes) before failure. The *UTS* and the *MOR* are the most important strength properties that represent lumber’s mechanical properties.

The symmetric proof load design [1] used a technique called proof loading. Proof loading refers to a process where specimens are subjected to only a modest load that breaks only the weakest pieces in a population. We used a scheme that tests a specimen up to a pre - set load and passes those that do not break at this load. In the symmetric proof load design, specimens are assigned into one of the two groups. One group is proof loaded in the *MOR* mode to a pre - determined proof load level, and the survivors are tested to failure in the *UTS* mode. The other group is done in a similar way, but this time proof loading is in the *MOR* mode. Our Summer – of – 2011 experiment conducted the symmetric proof load design experiment under three different proof load levels. The proof load levels are well spread out, which enables us to study the proof load effects on the strength of the proof load survivors. In addition to those proof loaded groups, the Summer – of – 2011 experiment also includes two shoulder groups where specimens are tested to failure in either the *MOR* or the *UTS* mode without any proof loading. The data collected from the shoulder groups allow us to determine the proof load levels for the proof loaded groups by estimating quantiles of the *UTS* distribution and the *MOR* distribution.

In this section, we introduce the Summer – of – 2011 experiment step by step, but do not provide the details of the analytic inputs required to conduct the Summer–of–2011 experiment. We refer the reader to Appendices A.1 and A.2 for the details.

The experimental materials came in three bundles of lumber: two bundles labelled #1 and #2 were of grade – type SPF 1650f-1.5E, while one labelled #3 was of type SPF No.2. Each 2 × 4 inch specimen was 12 feet long. SPF standards for Spruce, Pine and Fir species. The SPF 1650f-1.5E’s had

a design value of 1650 psi for the fibre stress in bending and an expected average *MOE* of 1.5 million psi. The SPF No.2s were No.2 grade lumber that came from a mixture of Spruce, Pine, and Fir species. Both grades were produced together from the same mill. The information about the mill is confidential. We selected SPF because it is Canada’s highest volume species group. Compared with the two bundles of 1650f-1.5E, the SPF No.2 bundle came from a population with generally weaker lumber strength properties. The inclusion of the SPF No.2 bundle added variation to the lumber strength properties, making the combined sample resemble to some small extent, a sample from the global population of all lumber of that grade.

Work began with a professional grader who examined each specimen visually and coded each specimen’s maximum strength – reducing characteristic (MSRC). The MSRC is a professional lumber grader’s best guess of the wood characteristics that will cause failure, and it is determined by visual inspection of the specimen. Examples of wood characteristics are “knots”, “grain” and “shake”. After the visual inspection, the investigators measured each specimen’s vibration modulus of elasticity (*MOE*) in accordance with ASTM D6874 [3]. The *MOE*, quantifying lumber’s stiffness, is measured by a non-destructive transverse vibration testing. Lumber specimens are simply supported by the machine’s two end points. One of those end points has a load cell transducer installed. The test starts with a gentle force pressing lumber specimens and releasing it immediately. As a result of the force, the lumber specimen vibrates. The load cell reads the specimen’s weight and frequency of oscillation into a personal computer that uses the reading to calculate the vibration *MOE*. However, the vibration *MOE* is affected by the lumber specimen’s moisture content. As a biological material, the surrounding moisture atmosphere affects the lumber specimen: it picks up some moisture in a humid environment and gives up some moisture to a dry environment. When lumber specimens are not well conditioned against moisture content, it is standard practice to adjust the vibration *MOE* for its moisture content. We used a moisture meter to estimate each lumber specimen’s MC. Given each lumber specimen’s vibration *MOE* and estimated MC, we calculated its adjusted vibration *MOE* following a standard procedure, ASTM D1990 (Appendix A.1).

Eight hundred and seventy specimens from the three bundles were divided into eight experimental groups based on the adjusted vibration *MOEs*: R20/40/60/100 and T20/40/60/100. The sorting was done bundle-by-bundle. For each bundle, the adjusted vibration *MOEs* were ranked from the largest

to the smallest, and the rank went from 1 to 290. The specimen with the  $i$ th rank was identified and labelled by  $ID(i)$  for  $i = 1, 2, \dots, 290$ . The specimens were then arranged by their ranks,  $ID(1), ID(2), \dots, ID(290)$ . The specimens from  $ID(1)$  to  $ID(10)$  were assigned one by one to T100, T100, T60, T40, T20, R20, R40, R60, R100 and R100 respectively. We repeated this procedure for the next 10 specimens, and so on until all 290 specimens were assigned. Thus, we created 29 blocks and 10 units within each block for each bundle (Table 1). Since the adjusted vibration  $MOE$  was highly correlated with lumber strength properties such as  $MOR$  and  $UTS$ , the groups T100, T60, T40, T20, R100, R60, R40, and R20 could be assumed to be homogenous in terms of the strength properties.

Table 1: The table shows schematically how the experimental groups used in the Summer – of – 2011 experiment were formed. Here,  $ID(i)$  is the identity of the lumber specimen with the  $i$ th rank in a given bundle.

Piece identifier	Rank	Group
ID(1)	1	T100
ID(2)	2	T100
ID(3)	3	T60
ID(4)	4	T40
ID(5)	5	T20
ID(6)	6	R20
ID(7)	7	R40
ID(8)	8	R60
ID(9)	9	R100
ID(10)	10	R100
ID(11)	11	R100
ID(12)	12	R100
ID(13)	13	R60
$\vdots$	$\vdots$	$\vdots$

Groups R60/40/20 and T60/40/20 were called the proof loaded groups (or single proof load design groups), where specimens were tested under different proof load levels in the  $MOR$  mode and in the  $UTS$  mode, respectively (details later). Each proof loaded group had 87 specimens. The experiment

had been designed to fail 60%, 40%, 20% of the specimens due to proof loading them in the *MOR* mode for the R60, R40, and R20 groups, respectively. As with the *MOR*, we expected 60%, 40%, 20% of the specimens would fail due to proof loading in the *UTS* mode for the T60, T40, and T20 groups, respectively. Groups R100 and T100 were called the “shoulder groups”, and each had 174 specimens. We called them shoulder groups because neither of the groups was proof loaded and instead the specimens in R100/T100 were loaded in a bending/tension machine respectively, and tested to failure.

The strength tests started with Groups T100 and R100. The *MOR* and *UTS* tests were conducted in accordance with American Standard Test Method (ASTM) D4761 [2] using specimens in R100 and T100, respectively. To measure a lumber specimen’s *MOR*, we load the specimen on a bending machine. The bending machine has two outermost support points that are 73.5 inches apart (the “test span”). The specimen is positioned between the two outermost support points so that its MSRC is randomly located within the test span. Once the bending test starts, two loading points that are equally spread out within the test span move upward at 2.8 inches per minute, and thus push the specimen upward with equal forces until the specimen fails (Figure 1). To measure a lumber specimen’s *UTS*, the specimen is loaded in a tension machine. The last two feet on both ends of the lumber specimen are then grabbed and pulled by the loading points of the tension machine in opposite directions parallel to the grain (Figure 2). The two loading points of the tension machine move at 0.5 inch per minute until the specimen fails.

The resulted data provided estimated quantiles of the *UTS* distribution and the *MOR* distribution, which allowed us to determine the proof load levels for the proof loaded groups R60/40/20 and T60/40/20 (Appendix A.2). Our goal was not to estimate the proof load levels precisely, but rather to obtain well separated proof load levels in order to investigate the proof load effects. Table 2 summarizes the estimated proof load levels in pounds, the estimated and the observed number of failed specimens due to proof loading, and the observed percentage of failed specimens due to proof loading for each experimental group R60/40/20 and T60/40/20. The proof load levels are spread well to give us the contrasts needed to study the proof load effects.

The specimens in R60/40/20 were proof loaded in the *MOR* mode. To proof load them, they were loaded on the bending machine, and the bending machine’s loading points moved at 2.8 inches per minute until the load reached 1770/1525/1237 pounds, respectively. If a specimen in R60/40/20

Figure 1: The bending machine conducts the destructive test for measuring *MOR*. The specimen is positioned between the two outermost support points. The two load points are spread equally within the test span to push the specimen upward with equal forces until failure.



Figure 2: The tension machine conducts the destructive test for measuring *UTS*. Once the machine is loaded with a specimen, it pulls the specimen in opposite directions at the loading points located at the two ends, until the specimen fails.





Table 2: The estimated proof load level (PLL) in pounds, the estimated and observed numbers of specimens failed due to the proof load and the observed percentage of failed specimens due to the proof load.

Groups	PLL (in lb)	# of Broken		Obs. % of Broken
		Est.	Obs.	
R60	1770	52	54	62
R40	1525	35	40	46
R20	1237	17	20	23
T60	25490	52	52	60
T40	20670	35	38	44
T20	15360	17	14	16

survived the proof loading procedure in the *MOR* mode, it was loaded to failure on the tension machine, and the tension machine’s loading points move at the rate of 0.5 inches per minute. As a result, for each specimen in Groups R60/40/20, we observed the *MOR* if it failed due to proof loading it in the *MOR* mode or *UTS* otherwise.

Similarly, each specimen in the T60/40/20 groups was proof loaded in the *UTS* mode, and the tension machine’s loading points moved at 0.5 inches per minute until the load reached 25490/20670/15360 pounds, respectively. If the specimen did not fail at the end of the proof loading procedure in the *UTS* mode, the surviving specimens of T60/40/20 were loaded to failure in the bending machine, and the bending machine’s loading points move 2.8 inches per minute. We observed *UTS* if the specimen failed due to proof loading in the *UTS* mode or *MOR* otherwise.

### 3 Exploratory analysis

We explore the major characteristics of *MOE*, *UTS* and *MOR* and their dependencies using the data collected from the shoulder groups T100 and R100. Group T100 has *MOE* and *UTS* measurements observed on the same specimen while Group R100 has *MOE* and *MOR* measurements observed on the same specimen. Section 3.1 presents the major characteristics of *MOE*, *UTS* and *MOR* (e.g. as seen in the empirical distribution functions that describe their characteristics well). Section 3.2 explores the dependencies

between *MOE* and *UTS*, and between *MOE* and *MOR*. Since *UTS* and *MOR* are not observed simultaneously on the same lumber specimen, our preliminary analysis is not sophisticated enough to explore the dependence between *UTS* and *MOR* directly. A companion paper [4] now in preparation presents approaches to assessing the dependence between two such random variables that cannot be observed simultaneously using the data collected from the proof loaded groups R60/40/20 and T60/40/20.

### 3.1 The *MOE*, *UTS* and *MOR* data

Table 3 lists the measured variables along with their units of measurement: *MOE* (kpsi), *UTS* (kpsi) and *MOR* (mpsi). Later in this section, we fit log – normal distributions to our samples for these three continuous variables. That means first rescaling their measurements to get unitless quantities, since the logarithm cannot be applied directly to measured quantities [7, 8]. More precisely *MOE* (mpsi) was divided by  $c$  (mpsi) where in accordance with a common practice we have selected  $c = 1$ . Other choices could have been made, for example to avoid numerical problems, but this choice proved satisfactory in our analysis. Thus the unitless version of an *MOE* measurement  $m_1$  (mpsi) is

$$\frac{m_1 \text{ mpsi}}{1 \text{ mpsi}} = \{m_1\}.$$

The *UTS* and *MOR* measurements were transformed in a similar way by dividing them by their units of measurement, namely kpsi. Hereafter, *MOE*, *UTS*, and *MOR* will refer to their unitless versions although to avoid notational clutter we drop the curly brackets  $\{\}$ . Note that the choice of  $c$  would not affect the appropriateness of the following analysis. Indeed, the following analysis would not change under a change in these units provided that unitless values are used consistently.

Table 3: Units for the continuous random responses *MOE*, *UTS*, and *MOR*.

Name	Group	Unit of measurement
<i>MOE</i>	R100 & T100	million psi (mpsi)
<i>UTS</i>	T100	thousand psi (kpsi)
<i>MOR</i>	R100	thousand psi (kpsi)

To visualize *MOE*, *UTS* and *MOR*, Figures 3 and 4 plot their histograms and boxplots, respectively. These plots suggest the population distributions of *MOE*, *UTS* and *MOR* are unimodal. We do not see strong evidence of asymmetries in the distributions for *MOR* and *MOE* but the *UTS* distribution seems positively skewed as would be consistent with a log – normal distribution.

Figure 3: Histograms of *MOR*, *UTS*, and *MOE*. The units of measurement for *MOR* and *UTS* are thousands of psi and that of *MOE* is in millions of psi.

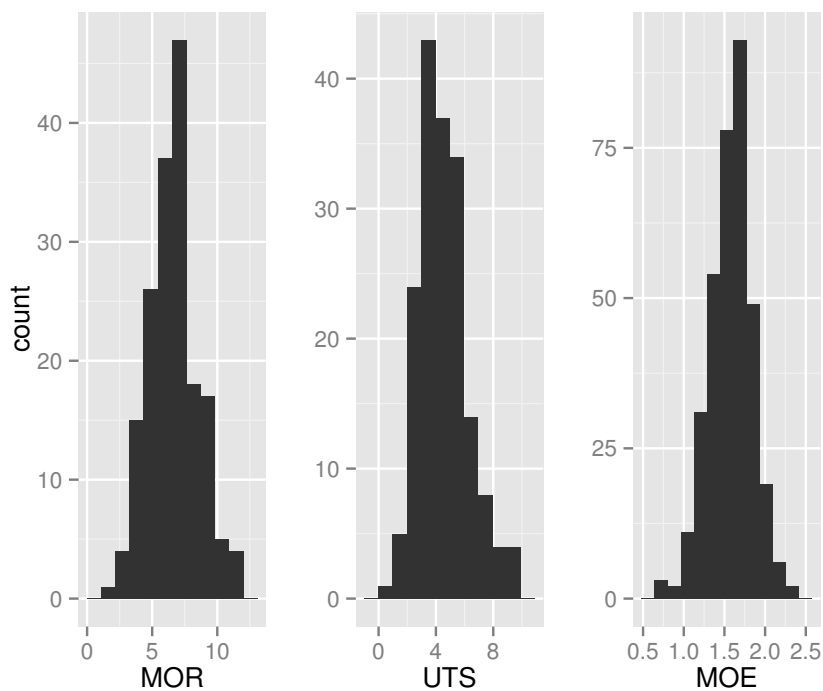
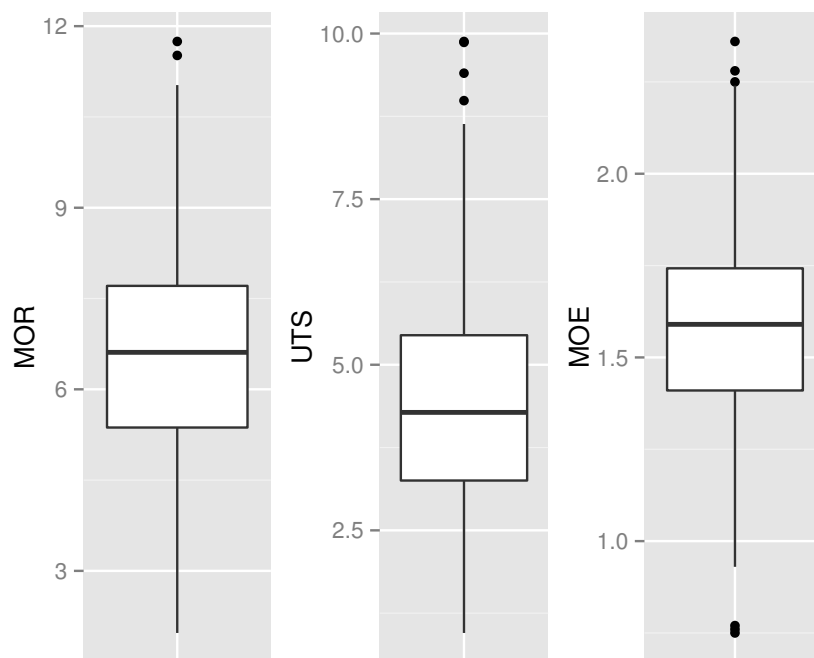


Figure 4: Boxplots of  $MOR$ ,  $UTS$ , and  $MOE$ . The lower and upper box boundaries are the 25<sup>th</sup> and the 75<sup>th</sup> percentiles ( $Q1$  and  $Q3$ ), respectively. Two vertical lines extend from the lower and upper box boundaries to the lower and upper whiskers, respectively. The lower whisker is  $1.5 \times (Q3 - Q1)$  from  $Q1$ . The upper whisker is  $1.5 \times (Q3 - Q1)$  from  $Q3$ . Observations not included between the whiskers are plotted with dots. The  $MOR$  and  $UTS$  are measured in thousands of psi,  $MOE$  is millions of psi.



Empirical quantiles are useful for investigating skewness. To confirm what we observe in Figures 3 and 4, we calculate the empirical quantiles of *MOR*, *UTS*, and *MOE*. The empirical distribution of a sequence of independent and identically distributed random variables  $\{X_1, X_2, \dots, X_n\}$  is defined as

$$\hat{F}_X(x) = \frac{1}{n} \sum_{i=1}^n I(X_i \leq x),$$

where  $I(\cdot)$  is the (0 or 1) indicator function. The inverse function of this discrete empirical distribution is defined as the empirical quantile function

$$\hat{Q}_X(t) = \hat{F}_X^{-1}(x) = \inf\{x : \hat{F}_X(x) \geq t\}.$$

The empirical quantiles of *UTS*, *MOR*, and *MOE* are summarized in Table 4, which suggests that the *MOE* and the *MOR* distributions are indeed approximately symmetric and the *UTS* distribution is slightly skewed to the right.

Table 4: Summary statistics for *MOE/UTS/MOR*: the 0<sup>th</sup> (min), 25<sup>th</sup>, 50<sup>th</sup>, 75<sup>th</sup> and 100<sup>th</sup> (max) empirical percentiles, the sample mean, and the sample standard deviation (SD). The sample size is N.

Name	Group	N	Empirical quantiles						SD
			Min	25%	Mean	50%	75%	Max	
<i>MOE</i>	R100&T100	348	0.75	1.40	1.58	1.59	1.74	2.36	0.27
<i>UTS</i>	T100	174	0.95	3.25	4.50	4.28	5.45	9.88	1.88
<i>MOR</i>	R100	174	1.97	5.28	6.62	6.61	7.62	11.75	1.71

To quantify the skewness observed in the empirical quantiles (Table 4) and Figures 3 and 4, we use the sample skewness measurement defined as

$$\frac{\sqrt{n(n-1)}}{n-2} \frac{\sum_{i=1}^n (x_i - \bar{x})^3 / n}{(\sum_{i=1}^n (x_i - \bar{x})^2 / n)^{3/2}},$$

for a sample of observations  $\{x_1, x_2, \dots, x_n\}$  from a random variable  $X$ . Table 5 gives the sample skewnesses of *MOE*, *UTS* and *MOR*. The *MOR* and *UTS* distributions are positively skewed while that of *MOE* is negatively skewed. To see if the skewnesses are significantly different from 0, we carry out the D'Agostino test of skewness [5] for each distribution. The null

hypothesis is that the skewness is zero, and the alternative, that the skewness is non – zero. The p – values are 0.23, 0.34, and 0.00 for the *MOE* distribution, the *MOR* distribution, and the *UTS* distribution, respectively. At the 5% significance level, the skewness of the *UTS* distribution is significantly different from zero while no significant skewness is found for *MOE* and *MOR*.

Table 5: Sample skewnesses for *MOE/UTS/MOR*. The sample size is N.

Name	Group	N	Skewness
<i>MOE</i>	R100&T100	348	-0.16
<i>UTS</i>	T100	174	0.73
<i>MOR</i>	R100	174	0.17

The Weibull distribution is commonly used to model lumber strength distributions [6]. It is a theoretical limit distribution for the minimum of a sequence of increasing length, of identically and independently distributed random variables, if the limiting distribution is non – degenerate. This fact is commonly used to justify the use of the Weibull distribution for modelling the failure time/strength where strength is determined by a “weakest link”. This makes the Weibull a plausible choice for the *UTS*’s probability distribution, since it is measured by applying an increasing uniform tensile stress along the longitudinal axis of the specimen lying within the test span and so it will ultimately be the strength of its weakest segment.

On the other hand, the Weibull is not the obvious choice for the *MOR* – there is no reason why a specimen should fail at the weakest segment since stress is not uniformly distributed over the specimen within the test span. In fact the *MOR* is commonly modelled by the log – normal or normal distribution [6].

The Weibull, log – normal and normal distributions vary from heavier to lighter tails. The density functions for these distributions are respectively: for the normal distribution,

$$f_{\text{normal}}(x; \mu_1, \sigma_1) = \frac{1}{\sigma_1 \sqrt{2\pi}} \exp \left\{ -\frac{(x - \mu_1)^2}{2\sigma_1^2} \right\}, \quad (1)$$

where  $\mu_1 \in (-\infty, \infty)$  and  $\sigma_1 > 0$ ; for the log – normal distribution,

$$f_{\text{logN}}(x; \mu_2, \sigma_2) = \frac{1}{x\sigma_2 \sqrt{2\pi}} \exp \left\{ -\frac{(\log x - \mu_2)^2}{2\sigma_2^2} \right\} \text{ for } x > 0, \quad (2)$$

where  $\mu_2 \in (-\infty, \infty)$  and  $\sigma_2 > 0$ ; and for the 2 – parameter Weibull distribution,

$$f_w(x; \beta, \eta) = \frac{\beta}{\eta} \left(\frac{x}{\eta}\right)^{\beta-1} \exp\left\{-\left(\frac{x}{\eta}\right)^\beta\right\} \text{ for } x \geq 0, \quad (3)$$

where  $\beta > 0$  and  $\eta > 0$ .

To find a distribution for the *MOE*, Figure 5 plots the empirical quantiles of *MOE* against the theoretical quantiles of the Weibull, the log – normal and the normal distributions. Similarly, Figures 6 and 7 give the quantile – to – quantile plots for *UTS* and *MOR*, respectively. If the theoretical quantiles were heavier than (respectively similar to, lighter than) the empirical quantiles, we would expect to see a concave downward (respectively linear, concave upward) curve.

Figure 5 thus points to a normal distribution or 2 – parameter Weibull distribution with a shape parameter of about 4 for modelling *MOE*. The log – normal distribution is too heavy tailed. Nevertheless in the sequel, we do fit the log – normal distribution for completeness. Figure 6 suggests the tails of the log – normal distribution are too heavy for the *UTS* but the 2-parameter Weibull distribution with a shape parameter of about 2 seems appropriate. Figure 7 suggests that a normal distribution or the 2-parameter Weibull distribution with shape parameter of about 4 seems an appropriate choice for modelling *MOR*.

Figures 5 to 7 suggest that each of the distributions, Weibull, log – normal and normal distributions could be appropriate in certain circumstances. So for completeness, we fit *MOR* (*UTS* and *MOE*) with the log – normal distribution together with the normal and the Weibull distributions.

We fit these three candidate distributions to the samples of *MOE/UTS/MOR*. Table 6 give the maximum likelihood estimates with standard errors for each parameter in each candidate distribution. Visualizing the results helps assess the adequacy of these three candidates as data descriptors so we plot their fitted cumulative distribution functions (CDFs) against their corresponding empirical CDFs. If the fitted CDF were close to the empirical CDF, the candidate distribution would be considered appropriate.

Figure 5: Sample quantiles of  $MOE$  against various theoretical quantiles. The normal theoretical quantiles are from a normal distribution with parameters  $\mu_1 = 0$  and  $\sigma_1 = 1$ . The log – normal theoretical quantiles are from a log – normal distribution with parameters  $\mu_2 = 0$  and  $\sigma_2 = 1$ .

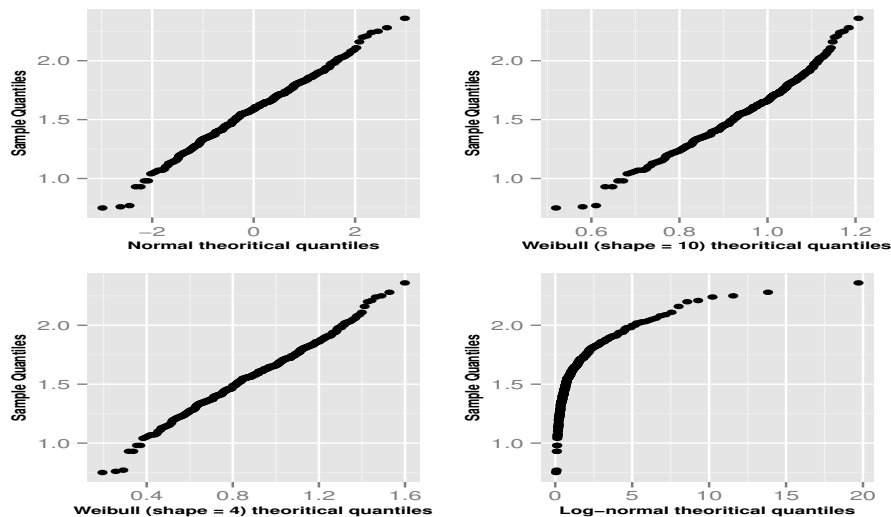


Table 6: Fitting the normal distribution, the 2-parameter Weibull distribution and the log – normal distribution to  $MOE/UTS/MOR$ . This table lists the maximum likelihood estimate of the parameter and its standard error.

		Weibull		normal		log – normal	
		$\beta$	$\eta$	$\mu_1$	$\sigma_1$	$\mu_2$	$\sigma_2$
$MOE$ (R100 and T100)	EST	6.56	1.69	1.58	0.27	0.44	0.18
	SE	0.26	0.01	0.01	0.01	0.01	0.01
$UTS$ (T100)	EST	2.79	5.05	4.50	1.71	1.43	0.40
	SE	0.16	0.15	0.13	0.09	0.03	0.02
$MOR$ (R100)	EST	3.85	7.32	6.62	1.87	1.85	0.31
	SE	0.22	0.15	0.14	0.10	0.02	0.02



Figure 6: Sample quantiles of  $UTS$  against various theoretical quantiles. The normal theoretical quantiles are from a normal distribution with parameters  $\mu_1 = 0$  and  $\sigma_1 = 1$ . The log-normal theoretical quantiles are from a log-normal distribution with parameters  $\mu_2 = 0$  and  $\sigma_2 = 1$ .

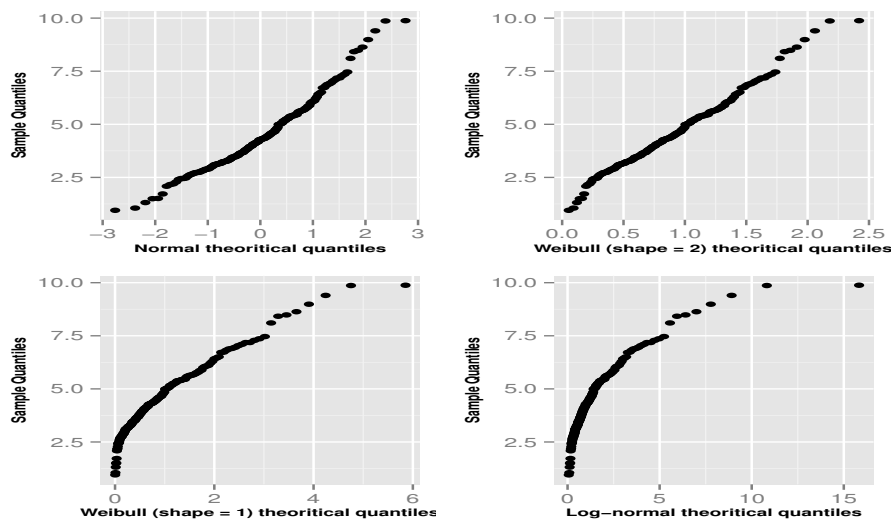


Figure 7: Sample quantiles of *MOR* against various theoretical quantiles. The normal theoretical quantiles are from a normal distribution with parameters  $\mu_1 = 0$  and  $\sigma_1 = 1$ . The log - normal theoretical quantiles are from a log - normal distribution with parameters  $\mu_2 = 0$  and  $\sigma_2 = 1$ .

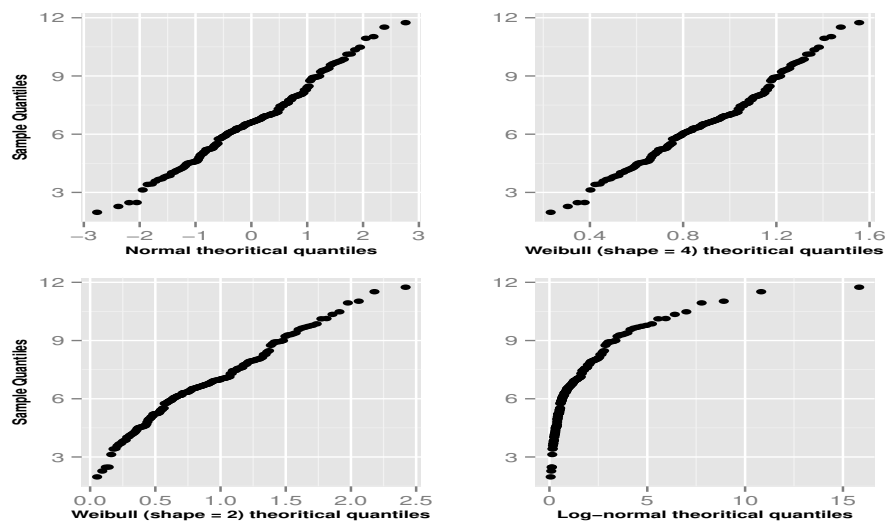
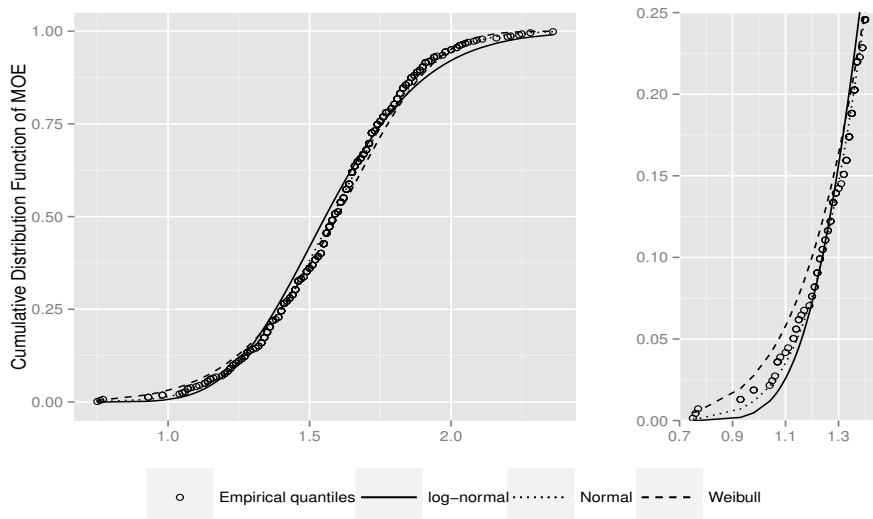


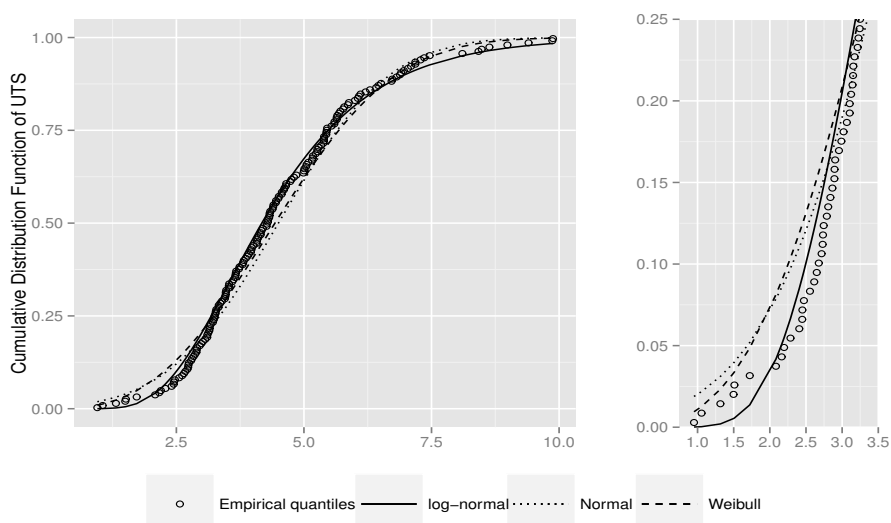
Figure 8 shows the CDFs of the *MOE* for the fitted normal, Weibull and log – normal cumulative distribution. The normal seems closest overall to the empirical CDF and hence seems best overall among the three candidates for *MOE*. However from the perspective of reliability, the left tail region is of paramount importance and that is shown in the right panel of Figure 8. Here again the estimated normal CDF seems best for *MOE* among the three candidates.

Figure 8: *MOE*. Left panel: the empirical cumulative distribution function (CDF) along with the fitted normal CDF with  $\hat{\mu}_1 = 1.58$  and  $\hat{\sigma}_1 = 0.27$ , the fitted Weibull CDF with  $\hat{\beta} = 6.56$  as well as  $\hat{\eta} = 1.69$  and the fitted log – normal CDF with  $\hat{\mu}_2 = 0.44$  and  $\hat{\sigma}_2 = 0.18$ . In the right panel we zoom in on the left tail region of the plots shown in the left panel. Observe that in both cases the fitted normal CDF seems best



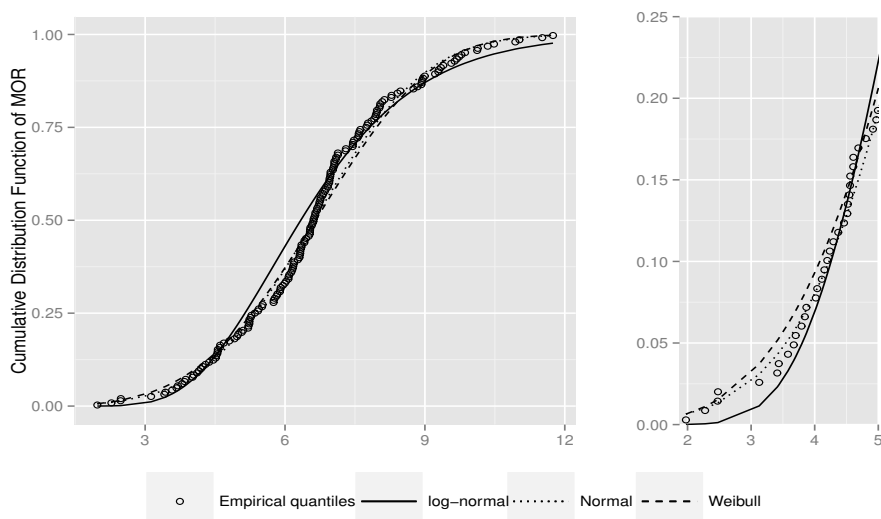
We repeat the previous exercise for the *MOE* but this time for the *UTS* with the results shown in Figure 9. The log – normal distribution seems best in this case, judging by the left hand panel of Figure 9. But the right panel suggests that Weibull provides the best fit to the very smallest quantiles of the *UTS* distribution but around the all important 5<sup>th</sup> quantile used in setting lumber design values the fitted log – normal and Weibull distributions are very close.

Figure 9: *UTS*. Left panel: the empirical cumulative distribution function (CDF), the fitted normal CDF with  $\hat{\mu}_1 = 4.50$  and  $\hat{\sigma}_1 = 1.71$ , the fitted Weibull CDF with  $\hat{\beta} = 2.79$  and  $\hat{\eta} = 5.05$ , and the fitted log – normal CDF with  $\hat{\mu}_2 = 1.43$  and  $\hat{\sigma}_2 = 0.40$ . In the right panel we again zoom in on the smallest quantiles and find that the Weibull fit is slightly better for the smallest percentiles but the log – normal distribution seems best at and above the 5<sup>th</sup> percentile.



Finally we turn to the *MOR* in Figure 10. Here the normal and Weibull distributions both seem appropriate and better than the log – normal even when considering the all important left tail of the distribution.

Figure 10: *MOR*. Left panel: the empirical cumulative distribution function (CDF) along with the fitted normal CDF with  $\hat{\mu}_1 = 6.62$  and  $\hat{\sigma}_1 = 1.87$ , the fitted Weibull CDF with  $\hat{\beta} = 3.85$  and  $\hat{\eta} = 7.32$  and the fitted log – normal CDF with  $\hat{\mu}_2 = 1.85$  and  $\hat{\sigma}_2 = 0.31$ . In the right panel we zoom in on the left tail region of the left panel and observe that the normal and Weibull are similar and both superior to the log – normal distribution.



To validate what we observe in Figures 8 – 10, we calculate the Akaike information criterion (AIC) for each fitted distribution. The AIC measures the distribution’s suitability for describing future data characteristics after penalizing for the number of parameters. It is defined as

$$AIC = 2 \times k_p - 2\ell,$$

where  $k_p$  is the number of parameters in the distribution, and  $\ell$  is the log – likelihood function evaluated at the maximum likelihood estimate. For all three candidate distributions,  $k_p = 2$ . We want to select a distribution with a small AIC value. Table 7 lists the AIC for the fitted normal, the fitted Weibull, and the fitted log – normal distributions of *MOE/UTS/MOR*.

Table 7: AIC values for the fitted normal, 2-parameter Weibull, and log – normal distributions for the *MOE/UTS/MOR* data. The criterion suggests the normal/log – normal/normal distributions for modelling *MOE/UTS/MOR*, respectively. However, in the latter two cases, the Weibull distribution is a close contender.

	AIC		
	normal	Weibull	log – normal
<i>MOE</i>	67.45	76.07	98.31
<i>UTS</i>	684.04	678.14	677.25
<i>MOR</i>	715.79	717.66	733.29

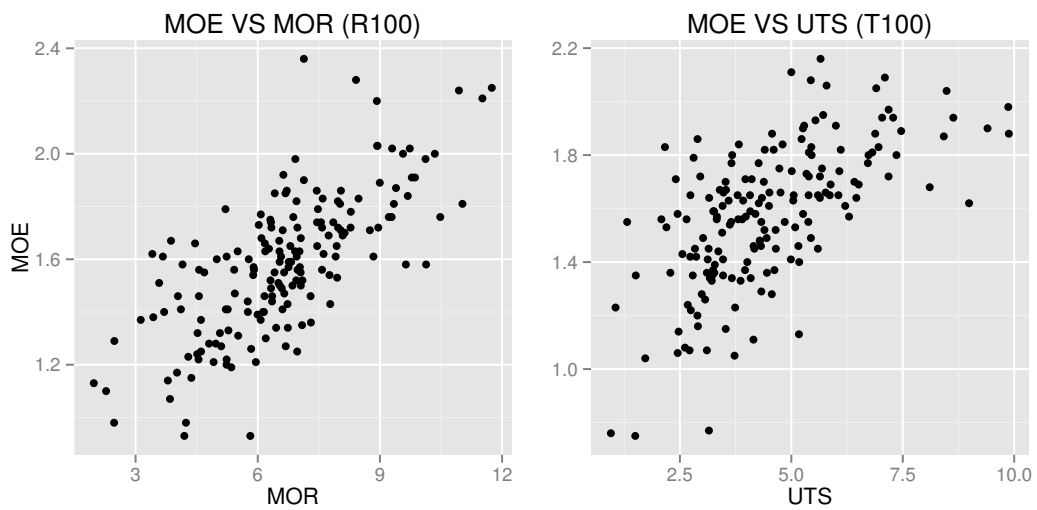
The AIC suggests using a normal distribution for modelling the *MOE* distribution, a Weibull or a log – normal distribution for modelling the *UTS* distribution and a normal or a Weibull distribution for modelling *MOR*. As noted above, the Weibull distribution may be more appropriate for modelling *UTS* based on theoretical arguments involving the weakest link.

### 3.2 Dependence between strength properties

In this subsection we turn to the all important topic of strength property relationships. The primary goals of the experiment went beyond merely learning the characteristics of the lumber strength properties for *MOE/UTS/MOR*, but also included the investigation of the dependencies among *MOE*, *UTS* and *MOR*. It was the latter goals that led to the complexity of our experimental design. Our preliminary analysis is not sophisticated enough to explore the dependence between *UTS* and *MOR* directly because *UTS* and *MOR* cannot be observed on the same specimen – that is left to a companion paper now in preparation. However, we do have paired observations of (*MOE*, *UTS*) from the shoulder group T100 and paired observations of (*MOE*, *MOR*) from the shoulder group R100. As noted above, *MOE* is known to be associated with *UTS* and *MOR*. To explore the potential association of *MOE* with either *UTS* or *MOR*, Figure 11 plots *MOE* against *MOR* (left panel) and *MOE* against *UTS* (right panel). Both *MOR* and *UTS* appear to be highly positively correlated with *MOE*.

Pearson’s correlation coefficient is used to evaluate linear association between two random variables, ranging between -1 and 1. A positive value means that the variables are positively correlated, which means they tend

Figure 11: Plots of  $MOE$  against  $MOR$  (left panel) and  $MOE$  against  $UTS$  (right panel). Both plots suggest a high positive correlation, although a non-linear relationship seems apparent in the right panel.



to be large and small together. A very high positive value (close to 1) implies a strong positive linear association between the two random variables. Similarly, a negative Pearson correlation coefficient means that the two variables have a negative linear relationship. A very negative Pearson correlation coefficient that is close to -1 implies a strong negative linear dependence. If the Pearson's correlation coefficient were 0, then there would be no linear dependence between the variables. The sample Pearson's correlation coefficient between two random variables  $X$  and  $Y$  with observations  $\{(x_i, y_i) \text{ for } i = 1, 2, \dots, n\}$  is

$$\frac{\sum_{i=1}^n (x_i - \bar{x})(y_i - \bar{y})}{\sqrt{\sum_{i=1}^n (x_i - \bar{x})^2 (y_i - \bar{y})^2}},$$

where  $\bar{x} = \sum_{i=1}^n x_i/n$  and  $\bar{y} = \sum_{i=1}^n y_i/n$ . The sample Pearson's correlation coefficients of  $(MOE, UTS)$  and  $(MOE, MOR)$  are 0.63 and 0.72, respectively. The pairs are strongly associated, linearly, confirming what we observe in Figure 11. The strong associations between  $MOE$  and the strength properties  $MOR$  and  $UTS$  provide justifies our use of the  $MOE$  to assign the specimens to the different experimental groups and hence to assume the experimental groups are homogenous in the strength properties described in Section 2.

Although we cannot easily visualize or quantify the dependence between  $UTS$  and  $MOR$  directly, the companion paper Cai and Zidek [4] presents a new theory that allows us to infer the stochastic dependence between these types of random variables.

## 4 Concluding remarks

The study of lumber's strength properties is important because it determines the reliability of a lumber structure under loads likely to be encountered in practice. Those loads in practice could come from such things as winds and seismic activity. We have introduced (Section 2) the Summer – of – 2011 experiment. The experiment was mainly designed and conducted to investigate relationship between  $MOR$  and  $UTS$ . We assigned 870 lumber specimens to 8 experimental groups based on the adjusted  $MOE$ s. Three major components formed the experimental groups: two shoulder groups without any proof loading, three groups proof loading in the  $UTS$  mode, and three groups proof loading in the  $MOR$  mode. Section 3 illustrates the



major characteristics of  $MOE$ ,  $UTS$ , and  $MOR$ . The exploratory data analysis suggests a normal distribution for modelling  $MOE$ , a Weibull or a log – normal distribution for modelling  $UTS$ , and a normal or a Weibull distribution for modelling  $MOR$ . The sample Pearson’s correlation coefficients of  $(MOE, UTS)$  and  $(MOE, MOR)$  indicate that  $MOE$  is strongly positively correlated with both  $UTS$  and  $MOR$ .

## A Appendices

### A.1 Adjusted MOE

Section 2 provided a detailed description of the Summer – of – 2011 Experiment. This appendix explains how the modulus of elasticity ( $MOE$ ) is adjusted for its moisture content (MC) and how we check whether the experimental groups are homogenous in terms of the lumber’s strength properties.

The  $MOE$  of each specimen is adjusted for its MC following a standard procedure, ASTM D1990. The adjustment for MC is conducted bundle by bundle. Let  $MC_{ij}$  be MC of the  $j$ th specimen of the  $i$ th bundle,  $MC_i$  be the average MC of the  $i$ th bundle, and  $MOE_{ij}$  be the MOE of the  $j$ th specimen of the  $i$ th bundle. The adjusted  $MOE$  of the  $j$ th specimen of the  $i$ th bundle is calculated as

$$\text{Adjusted } MOE_{ij} = MOE_{ij} \frac{1.857 - 0.0237 \times MC_i}{1.857 - 0.0237 \times MC_{ij}}.$$

Table 8 summarizes the sample mean and the sample standard deviation of the adjusted  $MOE$ ’s within each group for each bundle. The sample mean and the sample standard deviation of the adjusted  $MOE$ ’s across groups within each bundle are similar. For each group (T100/R100, T60/40/20, R60/40/20), we also combine all specimens from three bundles, and obtain the sample mean and the sample standard deviation of the adjusted  $MOE$ ’s of each group. The sample mean and the sample standard deviation of the adjusted  $MOE$ ’s across groups based on the combined bundles are also similar. Since the adjusted  $MOE$  is known to be highly correlated with other lumber strength properties such as  $MOR$  and  $UTS$ , the groups R100/60/40/20 and T100/60/40/20 are safely assumed to be homogenous in terms of the lumber’s strength.

Table 8: The sample mean and the sample standard deviation of the adjusted *MOE*'s in million pounds per square inch (psi) for each experimental group within each bundle and across three bundles. Bundles 1 and 2 are of grade – type SPF(Spruce, Pine, Fir) 1650f-1.5E. Bundle 3 is of type SPF No.2.

Bundle		T20	T40	T60	T100	R20	R40	R60	R100
1	Mean	1.66	1.66	1.66	1.66	1.66	1.67	1.67	1.67
	SD	0.23	0.24	0.24	0.24	0.23	0.23	0.24	0.24
2	Mean	1.64	1.64	1.65	1.64	1.64	1.64	1.64	1.64
	SD	0.23	0.23	0.21	0.24	0.23	0.23	0.23	0.24
3	Mean	1.43	1.43	1.43	1.43	1.44	1.44	1.44	1.45
	SD	0.26	0.26	0.26	0.27	0.27	0.27	0.28	0.28
1-3	Mean	1.59	1.59	1.59	1.59	1.59	1.59	1.59	1.59
	SD	0.27	0.27	0.27	0.27	0.27	0.27	0.27	0.27

## A.2 Estimating the proof load levels

The Summer – of – 2011 experiment was designed such that the proof loading procedure of R60/40/20 was expected to break 60%, 40%, 20% of the specimens, respectively. As with bending, we expected 60%, 40%, 20% of the specimens would break during proof loading procedures of T60/40/20, respectively. To achieve this, we estimated the 60%, 40%, 20% quantiles of the distributions of the modulus of rupture (*MOR*) and the ultimate tensile strength (*UTS*). The goal was not to estimate the proof load levels precisely, but rather obtain well separated proof load levels for us to estimate the proof load effects. Here, we only illustrate the quantile estimation procedure with the groups proof loading in the *MOR* mode because the quantile estimation procedure for the groups proof loading in the *UTS* mode is similar.

The Weibull distribution is commonly used to model the lumber strength properties such as *MOR* and *UTS*. The density of the 2-parameter Weibull distribution is

$$f_W(x; \beta, \eta) = \frac{\beta}{\eta} \left(\frac{x}{\eta}\right)^{\beta-1} \exp\left\{-\left(\frac{x}{\eta}\right)^\beta\right\} \text{ for } x \geq 0$$

where  $\beta > 0$  and  $\eta > 0$ . The quantile function of the 2-parameter Weibull distribution is

$$Q(p) = \eta (-\ln(1 - p))^{1/\beta}, 0 \leq p < 1. \quad (4)$$

The Weibull distribution is fitted to the *MOR* data collected from Group R100 using the maximum likelihood method. The maximum likelihood estimates of  $\beta$  and  $\eta$  and their standard errors are reported in Table 9. The maximum likelihood estimates are plugged into Equation 4 to obtain estimated quantiles  $\hat{Q}(p)$  of the *MOR* distribution.

Table 9: Maximum likelihood estimates of the Weibull parameters by fitting the R100 data with a Weibull distribution.

Parameter	Est	SE
Shape $\beta$	3.85	0.05
Scale $\eta$	7.32	0.02

The proof load levels of R60/40/20 are  $\hat{Q}(0.6)$ ,  $\hat{Q}(0.4)$  and  $\hat{Q}(0.2)$ , respectively. For a given  $p$ , the standard error (SE) of  $\hat{Q}(p)$  is obtained by the Delta method. The approximate 95% confidence interval of  $Q(p)$  is  $(\hat{Q}(p) \pm SE)$ . Table 10 lists the estimated quantiles and their standard errors together with the approximate 95% confidence intervals.

Table 10: Estimated quantiles of the *MOR* distribution with their standard errors (SE), and the approximate 95% confidence intervals (CI).

Quantile	Est	SE	95% CI of quantile
$Q(0.2)$	4.96	0.03	(4.62, 5.30)
$Q(0.4)$	6.15	0.03	(5.84, 6.46)
$Q(0.6)$	7.15	0.02	(6.85, 7.45)

We convert the estimated quantiles to the estimated numbers of specimens failed by the proof loading procedure, and convert the 95% confidence intervals of the quantile to the 95% confidence intervals of the number of failed specimens (Table 11). The proof loading procedure starts with R60, R40 and then R20. For R60, the proof loading procedure with the proof load level being the estimated quantile  $\hat{Q}(0.6)$  is expected to fail around 53 specimens ( $0.6 \times 87 = 52.2$ ). If the number of observed failed specimens at the end of the R60 proof loading procedure falls outside the 95% confidence interval of the number of failed pieces (47, 58), we treat it as a trigger alert and consider to revise our estimated proof load levels for R40 and R20.

Table 11: Estimated number of failed specimens of R60/40/20 with approximate 95% confidence intervals.

Group	# of Failed	
	Est.	CI
R20	18	(14, 22)
R40	35	(30, 41)
R60	53	(47, 58)

We are aware that the approximate 95% confidence interval of the quantile based on the Delta method may be wide, and decide to carry an additional approach to estimate the quantile and its corresponding 95% confidence interval. Previous FPInnovations *MOR* sample sets from the same mills suggest that the Weibull shape parameter  $\beta$  is about 4. We assume that *MOR* follows a Weibull distribution with scale parameter  $\eta$  and shape parameter of 4. The quantile function of a Weibull distribution with scale parameter  $\eta$  and shape parameter of 4 is

$$\eta(-\ln(1-p))^{1/4}.$$

Then *MOR*<sup>4</sup> follows an exponential distribution with scale parameter  $\lambda$  where  $\lambda = (1/\eta)^4$ . The approximate 95% confidence interval of  $1/\lambda$  is

$$\left( \frac{2 \times 174}{\hat{\lambda}\chi^2(0.975, 2 \times 174)}, \frac{2 \times 174}{\hat{\lambda}\chi^2(0.025, 2 \times 174)} \right),$$

where 174 is the number of specimens of R100 and  $\hat{\lambda}$  is the maximum likelihood estimate of  $\lambda$ . Since  $\eta$  is a function of  $\lambda$ , the 95% confidence interval of  $\eta$  is approximated by

$$\left( \frac{2 \times 174}{(1/\hat{\eta})^4\chi^2(0.975, 2 \times 174)}, \frac{2 \times 174}{(1/\hat{\eta})^4\chi^2(0.025, 2 \times 174)} \right),$$

where  $\hat{\eta} = \hat{\lambda}^{-1/4}$ . Thus the estimated quantile of *MOR* is

$$\hat{\eta}(-\ln(1-p))^{1/4},$$

and the approximate 95% confidence interval of the quantile is

$$\left( \frac{2 \times 174 \times (-\ln(1-p))^{1/4}}{(1/\hat{\eta})^4\chi^2(0.975, 2 \times 174)}, \frac{2 \times 174 \times (-\ln(1-p))^{1/4}}{(1/\hat{\eta})^4\chi^2(0.025, 2 \times 174)} \right).$$

Table 12 lists the estimated quantiles of the *MOR* distribution and the corresponding 95% confidence intervals. Table 13 presents the results of Table 12 in terms of the number of specimens failed by the proof loading procedure. The approximate 95% confidence intervals in Table 13 are narrower compared with the 95% confidence intervals in Table 11, which serves as a more conservative standard for monitoring the proof loading procedure.

Table 12: Estimated quantiles of the MOR distribution with 95% confidence intervals under the assumption that the shape parameter is 4.

Quantile	Est	95% CI of quantile
$Q(0.2)$	5.05	(4.87, 5.25)
$Q(0.4)$	6.21	(5.99, 6.46)
$Q(0.6)$	7.19	(6.94, 7.47)

Table 13: Estimated number of broken specimens of R60/40/20 with 95% confidence intervals.

Group	# of Broken	
	Est.	95% CI of number of broken pieces
R20	18	(16, 20)
R40	35	(32, 40)
R60	53	(48, 58)

## References

- [1] Amorim SD, Johnson RA (1986) Experimental designs for estimating the correlation between two destructively tested variables. *Journal of the American Statistical Association* 81(395):807 – 812
- [2] ASTM D4761 (2005) Standard test methods for mechanical properties of lumber and wood-based structural material. ASTM International, DOI: 10.1520/D4761-05
- [3] ASTM D6874 (2003) Standard test methods for nondestructive evaluation of wood-based flexural members using transverse vibration. ASTM International, DOI: 10.1520/D6874-03
- [4] Cai Y, Zidek JV (2015) Breaking the same board twice - again. In preparation
- [5] DAgostino R (1970) Transformation to normality of the null distribution of  $g_1$ . *Biometrika* 57(3):679 – 681
- [6] Gupta R, Gebremedhin KG, Grigoriu M (1986) Characterizing the strength of wood truss joints. *Transactions of American Society of Agricultural Engineers* 35(4):1285 – 1290
- [7] Massa L, Gubskaya AV, Knoll E (2011) Can one take the logarithm or the sine of a dimensioned quantity or a unit? Dimensional analysis involving transcendental functions. *Journal of Chemical Education* 88(1):67–70
- [8] Zhai Y (2011) Dynamic duration of load models. Master's thesis, Department of Statistics, University of British Columbia, British Columbia